Extended Abstracts of the 2015 International Conference on Solid State Devices and Materials, Sapporo, 2015, pp708-709

# Ultra-Sensitive 2D Photodetectors Based on Large-Scale Molybdenum Disulfide Crystals

Zhi-Peng Ling[1], Rui Yang[1], Jian-Wei Chai[2], Shi-Jie Wang[2], Yu Tong[1], Dian Lei[1], Qian Zhou[1], Xiao Gong[1], Dong-Zhi Chi[2], and Kah-Wee Ang[1,*]

[1] Silicon Nano Device Lab., Dept. of Electrical and Computer Engineering, National University of Singapore, Singapore 117582.

[2] Institute of Materials Research and Engineering, 3 Research Link, Singapore 117602.

[*] Phone: +65 6516-2575, Fax: +65 6779-1103, Email: angkw@ieee.org

## Abstract

**We report the demonstration of ultra-sensitive two-dimensional photodetectors based on large-scale (1x2 cm$^2$) $MoS_2$ crystals synthesized by magnetron sputtering. Excellent film uniformity and precise control of the $MoS_2$ thickness down to a monolayer (~0.75nm) were achieved. Using gold-free CMOS compatible processes, the photodetectors were realized with a wide spectral response from the visible to the near-infrared band. In particular, photodetectors with five $MoS_2$ monolayers exhibited high photoresponsivity of 1.8A/W, external quantum efficiencies exceeding 260%, and photo-detectivities of >10$^8$ Jones, surpassing the performance of mechanically exfoliated based photodetectors. Such synthesis approach shows promising scalability to wafer level in meeting the industrial requirements for optical communication applications.**

## 1. Introduction

Transition metal dichalcogenides materials such as molybdenum disulfide ($MoS_2$) have attracted great attention arising from the ability to isolate individual, atomically thin layers with unique electronic and optical properties from its bulk form. Previous approaches for obtaining thin $MoS_2$ layers include micromechanical exfoliation by scotch-tape [1] and chemical vapor deposition [2]. Among other challenges, these techniques are reported to have poor uniformity and repeatability in producing the desired film thickness and geometry.

This work addresses the above issues by using a physical vapor deposition (PVD) technique such as magnetron sputtering to synthesize highly uniform $MoS_2$ films with a precise control of thickness down to a monolayer over a large area (1x2 cm$^2$) substrate. Using gold-free CMOS compatible processes, $MoS_2$ photodetectors with ohmic contacts were demonstrated and method to enable further performance improvement was explored. Impressive optical response was achieved over a wide spectral range from the visible to the near-infrared band, which were shown to outperform the primitive 2D photodetectors fabricated by mechanical exfoliation.

## 2. Synthesis of Large Area $MoS_2$ Crystals

Our PVD synthesis involves the growth of atomically thin $MoS_2$ films by DC magnetron sputtering of Molybdenum target in a vaporized sulfur ambient, using a substrate temperature of 700°C, Sulfur partial pressure of $4.0 \times 10^{-7}$ millibars, Argon pressure of $6.0 \times 10^{-4}$ millibars and a low sputtering power of 6W [3]. Using this low sputtering power, the growth rate can be controlled to a high precision. The sputtered molybdenum atoms react with the vaporized sulfur atoms before landing onto the heated $HfO_2$ dielectric / silicon substrate to form $MoS_2$ layers (Fig. 1). Excellent thickness uniformity is demonstrated for 2ML $MoS_2$ from the matching Raman peaks on three independent locations along the film as shown in Fig. 2. Fig. 3 shows that similar to exfoliated $MoS_2$ films, the difference between the Raman peaks (Δ) corresponding to the in-plane $E_{2g}^1$ phonon mode and the out-of-plane $A_{1g}$ phonon mode increases with more layers. A precise control of the $MoS_2$ thickness is achieved, showing an average monolayer thickness of 0.75nm, and a low deviation of 5% (Fig. 4).

## 3. Device Fabrication

Fig. 5 shows the gold-free CMOS compatible fabrication process flow of the PVD-synthesized $MoS_2$ photodetector, in which ohmic contact is formed using titanium (Ti) metal electrodes fabricated via an evaporation and lift-off process. The final photodetector device structure is as shown in Fig. 6, whereby the performance is evaluated across a wide spectral range from the visible to the near-infrared band for varying film thicknesses and channel biases.

## 4. Results and Discussions

Fig. 7 and 8 show the improvements in photocurrent and thus the photoresponsivity with increasing number of $MoS_2$ layers. While the 2ML photodetector exhibits a photocurrent of ~10µA and a photo-responsivity of ~0.4A/W in the visible region, a significant increase by four times is achieved for the 5ML photodetector. Interestingly, although the exfoliated $MoS_2$ films generally show a blue shift of the optical bandgap with reducing layers, Fig. 8 shows that the PVD- synthesized $MoS_2$ photodetectors exhibit an extended optical absorption over a wide spectral range up to near-infrared (1200 nm) for all three investigated thicknesses (2ML, 3ML and 5ML), which is close to the bandgap of bulk $MoS_2$ [4]. One underlying mechanism could be attributed to the internal film strain commonly induced by the PVD synthesis [5],[6], which leads to a shrinkage in $MoS_2$ bandgap energy.

Fig. 9 shows the deconvolution of the measured XPS spectrum, in which the Mo and S peak binding energy positions and its linewidths are extracted. With increasing $MoS_2$ thickness, a clear shift in the S 2s peak binding energy position and linewidth is observed, which supports the presence of strain effect in the $MoS_2$ films (Fig. 10). Strain relaxation eventually occurs near the front surface in thicker $MoS_2$ film, as evident from the high RMS surface roughness (Fig. 11).

Even for an atomically thin 2ML photodetector, a high photodetectivity exceeding $10^9$ Jones is observed in Fig. 12, which outperforms the 3ML and 5ML photodetectors. This is primarily attributed to a significantly lower dark current in thinner $MoS_2$ films (Fig. 13). Fig. 14 shows the performance benchmarking of large scale $MoS_2$ photodetector demonstrated in this work over the exfoliated $MoS_2$, CVD $MoS_2$, and graphene based photodetectors [7-12]. Clearly, photodetectors enabled by large area $MoS_2$ synthesis show promising performance in addition to delivering better scalability.

Fig. 15 shows that increasing the channel bias not only enhances the charge collection efficiency, but also has the potential for causing carrier multiplication through impact ionization process due to a high electric field strength across the channel. This is confirmed from the external quantum efficiency (EQE) curves exceeding 100%. Furthermore, thicker $MoS_2$ layers are shown to benefit from increased photo-responsivity and EQE across all investigated channel bias (Fig. 16). Stable switching characteristics were also demonstrated on these $MoS_2$ photodetectors (Fig. 17), while Fig. 18 highlights further improvement in the rise and fall time with increasing channel bias.

## 5. Conclusion

Ultra-sensitive 2D photodetectors based on large-scale $MoS_2$ crystals were successfully demonstrated using gold-free CMOS compatible processes. Synthesized by magnetron sputtering, a precise control of the $MoS_2$ film thickness and uniformity was achieved over a large area substrate, with potential of scaling up to wafer level. The $MoS_2$ photodetectors were evaluated with a wide spectral response from the visible to the near-infrared band, showing great potential for optical communication applications.

## References

[1] K.S. Novoselov *et al.*, Proc. of the Natl. Academy of Sciences of the USA, 102 (2005) 10451-10453. [2] Q.H. Wang *et al.*, Nat Nano, 7 (2012) 699-712. [3] J. Tao *et al.*, Nanoscale, (2014). [4] K. K. Kam *et al.*, J. Phys. Chem., 86 (1982) 463-467. [5] D.M. Mattox, Handbook of Physical Vapor Deposition Processing, 2010, pp. 399-438. [6] L. Yang *et al.*, Sci. Rep., 4 (2014) 1-7. [7] Z. Yin *et al.*, ACS Nano, 6 (2011) 74-80. [8] W. Choi *et al.*, Adv. Materials, 24 (2012) 5832-5836. [9] F. Xia *et al.*, Nat Nano, 4 (2009) 839-843. [10] F. Xia *et al.*, Nano Lett., 9 (2009) 1039-1044. [11] S. H. Yu *et al.*, ACS Nano, 8 (2014) 8285-8291. [12] N. Perea-López *et al.*, 2D Materials, 1 (2014) 011004.

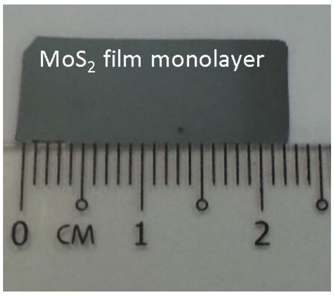


**Fig. 1.** Optical microscopy image of the PVD-synthesized $MoS_2$ films deposited on the $HfO_2$ / Silicon substrate.

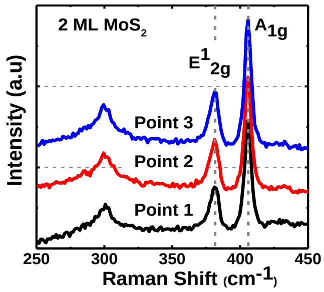


**Fig. 2.** Excellent film uniformity for PVD-synthesized $MoS_2$ films as thin as two monolayers.

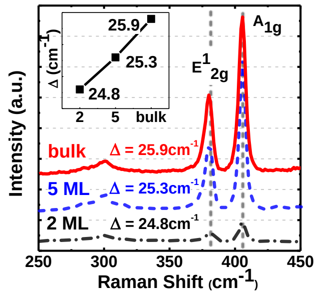


**Fig. 3.** Larger Raman $E^1_{2g}$ spectra peak shifts is observed with increasing number of $MoS_2$ layers.

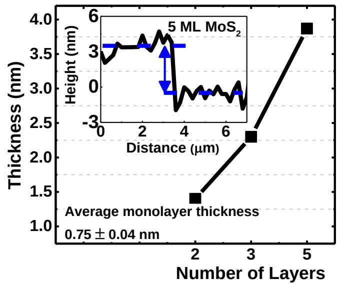


**Fig. 4.** Precise control of number of PVD-synthesized $MoS_2$ layers with low thickness deviation (~5%).

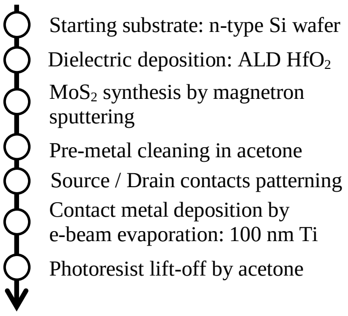


**Fig. 5.** Fabrication process flow of the PVD-synthesized $MoS_2$ photodetectors.

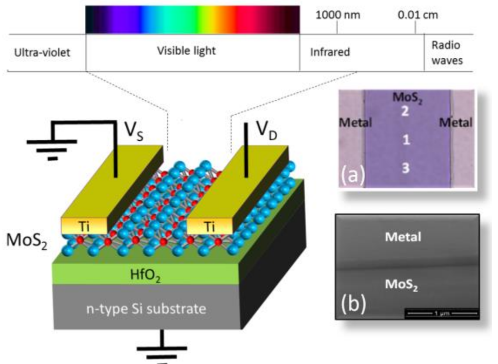


**Fig. 6.** Schematic of the $MoS_2$ photodetectors, evaluated across a wide spectral range from 400 nm to 1250 nm. Inset (a) and (b) show the optical and SEM micrograph image, respectively.

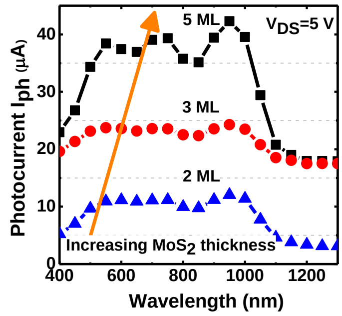


**Fig. 7.** Increasing photocurrent ($I_{ph}$) with increasing number of $MoS_2$ layers due to enhanced photo-absorption.

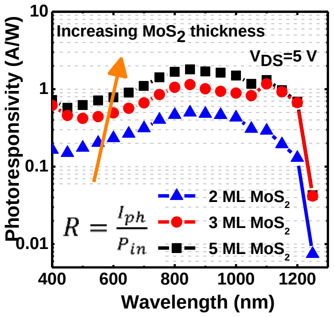


**Fig. 8.** Increasing photoresponsivity ($R$) is achieved with increasing number of $MoS_2$ layers.

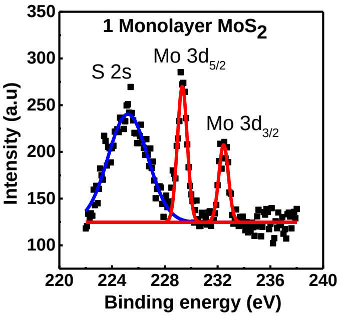


**Fig. 9.** A deconvolution of the XPS spectrum for the single monolayer $MoS_2$ film.

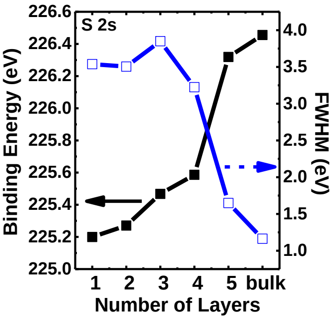


**Fig. 10.** S 2s peak binding energy position increases, and FWHM decreases as $MoS_2$ layer increases.

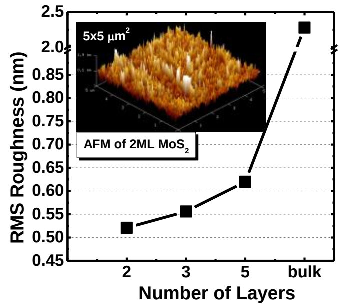


**Fig. 11.** RMS surface roughness increases with $MoS_2$ layers. Inset: 3D AFM image for the 2 ML $MoS_2$ film.

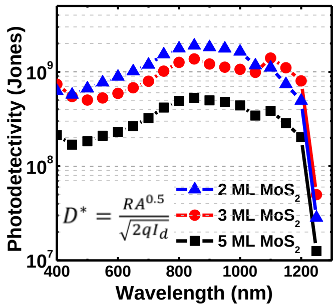


**Fig. 12.** Increased photodetectivity ($D^*$) with thinner $MoS_2$ layers due to lower dark current level.

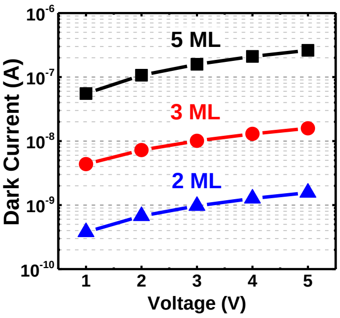


**Fig. 13.** Lower dark current ($I_d$) with thinner $MoS_2$ layers, giving rise to higher photodetectivity.

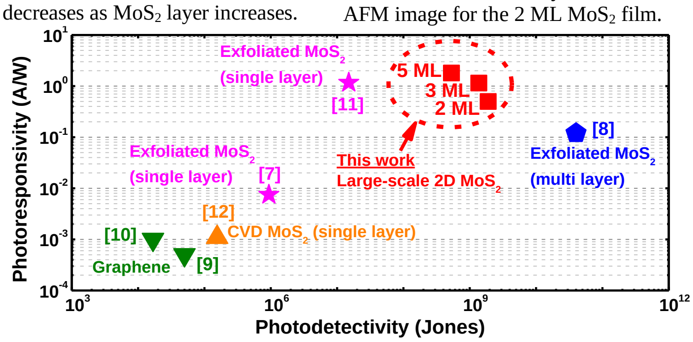


**Fig. 14.** The PVD-synthesized $MoS_2$ photodetectors demonstrated in this work outperform the previously reported $MoS_2$ photodetectors based on mechanical exfoliation, and CVD techniques, as well as Graphene-based photodetectors.

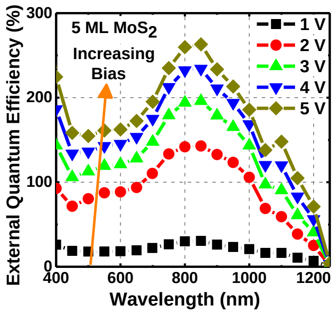


**Fig. 15.** Increasing external quantum efficiency with increasing applied bias across a wide spectra region.

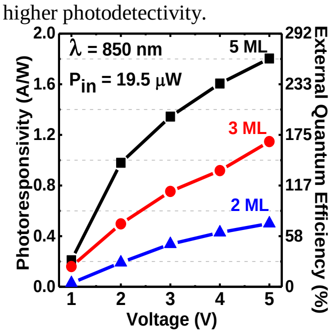


**Fig. 16.** Increasing bias leads to higher $R$ and $EQE$, which enhances further with thicker $MoS_2$ layers.

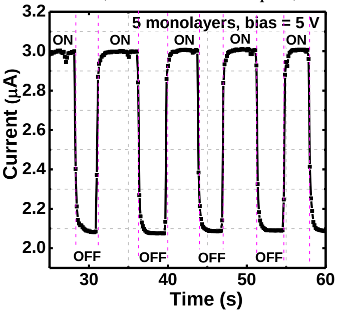


**Fig. 17.** A stable switching characteristics of the PVD-synthesized $MoS_2$ photodetector.

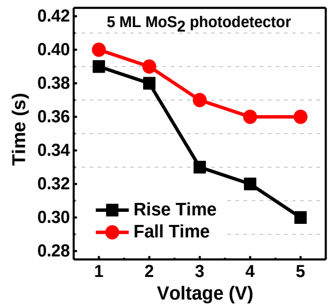


**Fig. 18.** Increasing channel bias reduces the rise and fall time of the $MoS_2$ photodetector.